AD-A070 540 NAVAL OCEAN SYSTEMS CENTER SAN DIEGO CA F/G 17/1

LIKELIHOOD FILTERING OF PASSIVE AMBIGUITY SURFACES.(U)

FEB 79 S J MCCARTHY

UNCLASSIFIED NOSC/TR-408 NL

1 OF 1

AD

A070540

END

DATE

FILMED

8 79

DDC

LEVEL II

12

NOSC

DDC RECEIVED JUN 28 1979

NOSC TR 408

NOSC TR 408

ADA070540

Technical Report 408

LIKELIHOOD FILTERING OF PASSIVE AMBIGUITY SURFACES

S. J. McCarthy

February 1979

Prepared for
Naval Electronic Systems Command

DDC FILE COPY

This document has been approved for public release and sale; its distribution is unlimited.

ORIGINAL CONTAINS COLOR PLATES: ALL DDC REPRODUCTIONS WILL BE IN BLACK AND WHITE.

NAVAL OCEAN SYSTEMS CENTER
SAN DIEGO, CALIFORNIA 92152

79 06 27 005

NAVAL OCEAN SYSTEMS CENTER, SAN DIEGO, CA 92152

AN ACTIVITY OF THE NAVAL MATERIAL COMMAND

RR GAVAZZI, CAPT, USN
Commander

HL BLOOD
Technical Director

ADMINISTRATIVE INFORMATION

The work in the report was sponsored by the Naval Electronic Systems Command, NELEX-320 under Program Element 61153N Subproject XR02105502. Funding being provided by the Office of Naval Research. Work was performed from December 1977 through September 1978.

Released by
DA HANNA, Head
Signal Processing and
Display Division

Under authority of
HA SCHENCK, Head
Undersea Surveillance
Department

The views and conclusions contained in this report are those of the author and should not be interpreted as necessarily representing the official policies, either expressed or implied, of the U.S. Government.

UNCLASSIFIED

SECURITY CLASSIFICATION OF THIS PAGE (When Data Entered)

REPORT DOCUMENTATION PAGE		READ INSTRUCTIONS BEFORE COMPLETING FORM
1. REPORT NUMBER NOSC Technical Report TR 408 (TR 408)	2. GOVT ACCESSION NO.	3. RECIPIENT'S CATALOG NUMBER
4. TITLE (and Subtitle) 6 LIKELIHOOD FILTERING OF PASSIVE AMBIGUITY SURFACES		9 5. TYPE OF REPORT & PERIOD COVERED Research report Dec 1977 - Sep 1978
		6. PERFORMING ORG. REPORT NUMBER
7. AUTHOR(s) 10 S. J. McCarthy		8. CONTRACT OR GRANT NUMBER(s)
9. PERFORMING ORGANIZATION NAME AND ADDRESS Naval Ocean Systems Center San Diego, CA 92152 393 159		10. PROGRAM ELEMENT, PROJECT, TASK AREA & WORK UNIT NUMBERS 61153N, XR02105502
11. CONTROLLING OFFICE NAME AND ADDRESS Naval Electronic Systems Command Washington, D.C.		11 12. REPORT DATE February 1979
		13. NUMBER OF PAGES 34
14. MONITORING AGENCY NAME & ADDRESS (if different from Controlling Office) 12 34 p.		15. SECURITY CLASS. (of this report) Unclassified
		15a. DECLASSIFICATION/DOWNGRADING SCHEDULE
16. DISTRIBUTION STATEMENT (of this Report) Approved for public release; distribution unlimited 14 NOSC/TR-408		
17. DISTRIBUTION STATEMENT (of the abstract entered in Block 20, if different from Report) 16 XR02105 17 XR0210550 2		
18. SUPPLEMENTARY NOTES		
19. KEY WORDS (Continue on reverse side if necessary and identify by block number) Sonar Signal Processing Spectral Analysis Adaptive Filtering		

20. ABSTRACT (Continue on reverse side if necessary and identify by block number)

The likelihood ratio techniques for conducting cross-correlation processing under conditions of unknown signal and noise spectral properties are investigated. The forms of the likelihood ratio processors are presented and their statistics developed. The statistics, in the form of receiver operating characteristics, are used to compare the likelihood ratio techniques against a normalized cross correlation. The likelihood ratio techniques are shown to be advantageous if the spectral properties of either the signal or the noise vary across the processing bandwidth.

393 159

DD FORM 1 JAN 73 1473 EDITION OF 1 NOV 65 IS OBSOLETE
S/N 0102-LF-014-6601

UNCLASSIFIED

SECURITY CLASSIFICATION OF THIS PAGE (When Data Entered)

CONTENTS

Accession For
NTIS GRA&I
DDC TAB
Unannounced
Justification
By
Distribution/
Availability Codes
Dist | Avail and/or special
A

1.0 INTRODUCTION

Cross-correlation calculations of signals received by two different sensors can be employed for estimation of position and velocity parameters of the transmitting source. These same calculations can be employed as a normalized detection statistic through the use of coherence or regression of one sensor's output with respect to the other. Independent of whether the calculations are primarily for estimation or detection purposes, filtering of the received signals should be conducted in a fashion to optimize performance. If full knowledge of the noise statistics exists for each sensor as well as the statistics of the received signals, then the procedure for optimizing* the filtering can be found in Refs. 1 through 4. For detection purposes, the processor is based upon the likelihood ratio, which declares a signal present if

$$\frac{P(\overline{X} \mid \text{signal plus noise})}{P(\overline{X} \mid \text{noise})} \geqslant T \tag{1}$$

where $\overline{X}$ denotes the data of observation, $P(\overline{X} \mid Z)$ denotes the probability of the input data occurring under hypothesis Z, and T denotes a threshold corresponding to a particular probability of false alarm.† For parameter estimation, the processor is based upon the maximum likelihood solution

$$\frac{\partial}{\partial\theta} P(\overline{X} \mid \text{signal plus noise}) = 0 \tag{2}$$

where θ is the unknown parameter. In situations where little *a priori* knowledge exists about the noise and signal statistics, optimization of the processing is not as straightforward. The concept of a likelihood ratio processor is still advantageous, but now sampled or approximated values have to be utilized in the likelihood ratio instead of true values. The use of sampled values in the likelihood ratio to describe unknown values can be thought of as single-iteration adaptive filtering of the cross-correlation calculation. With two sensors being involved in the calculations, the adaptation need not be constrained to the individual signals at each sensor but can occur on the cross-correlation or equivalently, the cross-spectrum calculated between the sensors. As will be shown in this report, adaptation on the cross-spectrum by means of a likelihood expression provides a formalism for matching the processing bandpass to the bandwidth of the signal and for compensating for colored noise or interference within the processing bandpass. One of the major advantages of the adaptation

---

*Optimization here refers to maximizing the probability of detection for a given probability of false alarm (i.e., the Neyman-Pearson criteria) and providing minimum variance parameter estimates (the asymptotic property of maximum likelihood estimators).

[1]W.J. Bangs, "Array Processing With Generalized Beam-Formers," Ph.D. Dissertation, Yale University, New Haven, Connecticut, September 1971.

[2]C.W. Helstrom, *Statistical Theory of Signal Detection*, Permagon Press, 1968.

[3]H.L. Van Trees, *Detection, Estimation, and Modulation Theory, Part I*, John Wiley and Sons, 1968.

[4]D. Middleton, *An Introduction to Statistical Communication Theory*, McGraw-Hill, 1960.

†A bar notation is used to denote vectors.

is that no *a priori* assumptions about the nature of the signals (broadband or narrowband) or the interference has to be made.

The purpose of the work presented in this report is to present the statistics for algorithms based on likelihood criteria (likelihood ratio or maximum likelihood) that adapt on the cross-spectrum in order to jointly detect and estimate signal parameters. Section 2 of the report will discuss the algorithms examined while Section 3 will describe their statistical properties. Finally, Section 4 presents the conclusion.

2.0 LIKELIHOOD EXPRESSIONS FOR CROSS-CORRELATION PROCESSING

Two likelihood-based algorithms for joint detection and estimation of signal parameters from data at the output of two sensors will be considered in this report. The first is a generalized likelihood ratio test statistic, while the other is an approximate form of a maximum likelihood parameter estimator. Selection of these two algorithms is based on their being likelihood processors and on their being normalized test statistics. A normalized test statistic does not depend upon absolute power levels received at the sensors. For low-frequency acoustic signals, where the noise background has been shown to be stationary for only short time periods, this property takes on added importance (Ref. 5).

GENERALIZED LIKELIHOOD EXPRESSION

A generalized likelihood ratio test statistic is the classical approach (Refs. 2, 3, 6) for detecting a signal when full knowledge about the signal or noise properties is not available. For cross-correlation processing, these properties are the signal time-difference between the sensors, the signal-frequency difference between the sensors, the spectral level of the signal as a function of frequency, and the spectral level of the noise as a function of frequency. The test statistic has the form

$$\Lambda_{GLR} = \frac{p(\overline{z}|\overline{\theta}_1)\{\text{max. over } \overline{\theta}_1\}}{p(\overline{z}|\overline{\theta}_0)\{\text{max. over } \overline{\theta}_0\}} \tag{3}$$

where $p(\overline{z}|\overline{\theta})$ represents the conditional density of the input data on the parameter set $\overline{\theta}$, $\overline{\theta}_1$ denotes the parameter set under condition of signal plus noise being present, and $\overline{\theta}_0$ denotes the parameter set under the condition of noise only being present. The above test statistic forms maximum likelihood estimates for both $\overline{\theta}_1$ and $\overline{\theta}_0$ and substitutes these into the likelihood ratio as if they were the true values. The above test statistic has been derived for the case where the signal and noise are assumed to be Gaussian distributed, but their respective spectral levels as a function of frequency are unknown. Also, the signal's time difference and frequency difference between the sensors is assumed unknown. The

[5] T. Arase and E. Arase, "Deep Sea Ambient Noise Statistics," *J. Acoust. Soc. Am.*, Vol. 44, pp. 1679-1684, April 1968.

[6] D. Becker, "Investigate the Use of Alternate Sample Statistics," ORINCON Company Report, prepared under Contract N000123-76-C-0505, December 1976.

derivation of the test stastic under these conditions is discussed in Refs. 6 and 7. A condensed form of the derivation is presented in Appendix A and leads to*

$$\Lambda_{GLR}(\tau) = \sum_{k \epsilon K} \ln\left\{1 - \hat{\gamma}^2(w_k) \cos^2 [w_k\tau + \hat{\psi}(w_k)]\right\}. \tag{4}$$

Here, $\hat{\gamma}^2(w_k)$ is the sampled magnitude squared coherence (MSC) between the two sensors at radian frequency w_k, $\hat{\psi}(w_k)$, is the sampled cross-spectral phase between the two sensors at radian frequency w_k, τ is the search parameter over the time difference between the sensors, and K is the set of frequencies over which filtering is to be performed.† Equation (4) shows that a sum of information across frequency is taken, but the summation posses-ses a complicated dependence on the sampled cross-spectral and auto-spectral parameters. Use of Eq. (4) does not necessarily guarantee that the two-sensor probability of detection will be maximized or that minimum variance parameter estimates will occur. The use of Eq. (4) can only be expected to provide nearly optimum detection performance because the general concept of a likelihood ratio processor has been retained. Also, since the parameter estimates are maximum likelihood estimates, they approach minimum variance estimates asymptotically as a function of observation time (Ref. 9).

MAXIMUM LIKELIHOOD ESTIMATOR (APPROXIMATE)

Since a generalized likelihood ratio processor does not necessarily guarantee optimum processing performance, it is reasonable to consider other likelihood-based processing techniques. This consideration can be based upon ease of implementation among other factors. The maximum likelihood estimate for the set of signal parameters $\bar{\theta}_1$ is given by the solution of

$$p(\bar{r}|\bar{\theta}_1) \text{ (max. over } \bar{\theta}_1). \tag{5}$$

In Eqs. (3) and (4), it was assumed that $\bar{\theta}_1$ included the noise spectral levels as a function of frequency and the signal spectral levels as a function of frequency. If the signal and noise spectral levels as a function of frequency are known, Eq. (5) leads to (Refs. 10, 11)

$$\Lambda_{ML}(\tau) = \sum_{k \epsilon K} \frac{\gamma^2(w_k)}{1 - \gamma^2(w_k)} \frac{|\hat{G}_{12}(w_k)|}{|G_{12}(w_k)|} \cos [w_k\tau + \hat{\psi}(w_k)] \tag{6}$$

---

*The maximization of Λ_{GLR} over the frequency difference between the sensors is implicit in equation 4. It is further assumed that a narrowband Doppler correction is sufficient such that the maximizations over the Doppler and time-difference parameters are asymptotically independent of each other (Ref. 8).

†The ∧ notation is used to denote sampled parameters as opposed to true parameters.

[7] Reference available to qualified requesters.

[8] P.M. Schultheiss, "Estimation of Doppler Shift and Differential Doppler Shift," Yale University, Technical Report, prepared under Contract N66001-76-C-1082, June 1977.

[9] H. Cramer, *Mathematical Methods of Statistics*, Princeton University Press, 1946.

[10] G. Carter, "Time Delay Estimation," NUSC TR 5335, April 1976.

[11] E. Hannan and J. Thompson, "Estimating Group Delay," *Biometrika*, Vol. 60, pp. 241-253, 1973.

where $\gamma^2(w_k)$ represents the true value of MSC, $G_{12(w_k)}$ represents the true cross-spectral power, $\hat{G}_{12(w_k)}$ represents the sampled cross-spectral power, and τ, $\hat{\psi}(w_k)$, and K are as defined earlier. If sampled spectral properties are substituted for true spectral properties in Eq. (6), the resulting processor is given by

$$\Lambda_{AML}(\tau) = \sum_{k\epsilon K} \frac{\hat{\gamma}^2(w_k)}{1-\hat{\gamma}^2(w_k)} \cos\,[w_k\tau + \hat{\psi}(w_k)]\,. \tag{7}$$

This relationship represents an inverse transform of the cross-spectral phase with a weighting at each frequency dependent upon the sampled MSC. Equation (7) possesses the following properties: it represents a normalized detection statistic, it is a zero mean test statistic with noise only present [as opposed to Eq. (4)], and it can be implemented using FFT processing techniques. It should be stated that use of Eq. (7) as a detection statistic was not rigorously derived.

LOW COHERENCE PROPERTIES OF THE LIKELIHOOD EXPRESSIONS

The form of the generalized likelihood ratio test stastic and the approximate maximum likelihood estimator can be examined for the case of low input coherence levels. This assumption simplifies the form of each algorithm such that the difference between them becomes more apparent. Assuming low input coherence levels, the first-order terms describing Eqs. (4) and (7) are

$$\Lambda_{GLR} \approx \sum_{k\epsilon K} \hat{\gamma}^2(w_k) \cos^2 [w_k\tau + \hat{\psi}(w_k)] \tag{8}$$

$$\Lambda_{AML} \approx \sum_{k\epsilon K} \hat{\gamma}^2(w_k) \cos\,[w_k\tau + \hat{\psi}(w_k)]. \tag{9}$$

These expressions differ only in the manner in which the cross-spectral phase is combined across frequency. The weighting applied to each cross-spectral phase measurement is identical. If the cosine squared term of Eq. (8) is written in terms of the twice-angle formula,

$$\Lambda_{GLR} \approx \frac{1}{2} \sum_{k\epsilon K} \hat{\gamma}^2(w_k) + \frac{1}{2} \sum_{k\epsilon K} \hat{\gamma}^2(w_k) \cos\,[2w_k\tau + 2\hat{\psi}(w_k)], \tag{10}$$

the difference between the two algorithms can also be interpreted in the following sense: the generalized likelihood test statistic uses both a coherent and incoherent summation of information across frequency, and for wideband signals the generalized likelihood expression requires a higher degree of consistency in the cross-spectral phase measurements across frequency.

Equations (8) and (9) allow a simple interpretation of the manner in which both algorithms act as adaptive filters on the cross spectrum. The contribution from each frequency region does not depend on absolute spectral levels but only upon the measured coherence between the sensors at each frequency. If low coherence is detected in particular frequency regions, those regions are weighted less than other frequency regions.

ENVELOPE FORM OF THE ALGORITHMS

The two sensor test statistics defined by Eqs. (4) and (7) are basically wideband processing algorithms. Equivalent performance on a narrowband signal can be obtained, with a large reduction in processing load, by using envelope versions of these algorithms. The envelope expressions are straightforward for the low-coherence form of both algorithms

$$\Lambda_{GLR} \Rightarrow \frac{1}{2} \sum_{k \epsilon K} \hat{\gamma}^2(w_k) + \left| \frac{1}{2} \sum_{k \epsilon K} \hat{\gamma}^2(w_k)\, e^{i[2w_k\tau + 2\hat{\psi}(w_k)]} \right| \tag{11}$$

$$\Lambda_{AML} \Rightarrow \left| \sum_{k \epsilon K} \hat{\gamma}^2(w_k)\, e^{i[w_k\tau + \hat{\psi}(w_k)]} \right| \tag{12}$$

but are more difficult to write for the exact expressions. That is, an explicit form for the envelope of Λ_{AML} can be written as

$$\Lambda_{AML} = \left| \sum_{k \epsilon K} \frac{\hat{\gamma}^2(wk)}{1 - \hat{\gamma}^2(w_k)}\, e^{i[w_k\tau + \hat{\psi}(w_k)]} \right| \tag{13}$$

but no explicit form for the envelope of Λ_{GLR} is known. In order to realize the envelope properties of Λ_{GLR}, Eq. (4) was sampled densely over one cycle of the bandpass center frequency and the maximum value selected. This procedure was repeated at τ intervals corresponding to the reciprocal of twice the processing bandwidth.

3.0 STATISTICS FOR THE TWO-SENSOR LIKELIHOOD EXPRESSIONS

In order to effectively evaluate the performance of the likelihood expressions, the statistics for each expression must be determined. The number of summation terms across frequency in these expressions in general will not be large enough to justify central limit theorem approximations. For general use, the statistics of Λ_{GLR} and Λ_{AML} need to be derived from the joint probability distribution of $\hat{\gamma}^2$ and $\hat{\psi}$. Due to the nonlinear dependence of Eqs. (4) and (7) with respect to $\hat{\gamma}^2$ and $\hat{\psi}$, exact determination of the statistics for Λ_{GLR} and Λ_{AML} is difficult. The low level coherence forms of both algorithms are considerably simpler though and it is generally the low signal-to-noise ratio properties of algorithms that are of the most interest. That is, the probability of false alarm (P_{FA}) is controlled by the zero-coherence level properties and the probability of detection (P_D) is controlled by low-level coherence except in the region where detection probabilities are approaching unity.

In this section, the statistics for the low-level coherence forms of Λ_{GLR} and Λ_{AML} will be developed. These statistics are governed by the probability distribution of $\hat{\gamma}^2(w_k)$ and $\hat{\psi}(w_k)$ where these random variables are defined by

$$\hat{\gamma}^2(w_k) = \frac{\left| \sum_{n=1}^{N} F(w_k, n)\ H^*(w_k, n) \right|^2}{\left| \sum_{n=1}^{N} F(w_k, n)\ F^*(w_k, n) \right| \left| \sum_{n=1}^{N} H(w_k, n)\ H^*(w_k, n) \right|} \tag{14}$$

$$\hat{\psi}(w_k) = \arctan \left\{ \frac{\mathrm{I\ mag} \left[\sum_{n=1}^{N} F(w_k, n)\ H^*(w_k, n) \right]}{\mathrm{Rl} \left[\sum_{n=1}^{N} F(w_k, n)\ H^*(w_k, n) \right]} \right\} . \tag{15}$$

Here, $F(w_k, n)$ denotes the Fourier transform at the n^{th} time interval taken from sensor one at radian frequency w_k, and $H(w_k, n)$ denotes the Fourier transform at the n^{th} time interval taken from sensor two at radian frequency w_k. If the noise at each sensor is constrained to be jointly Gaussian and independent, the signal is a Gaussian random variable, and the transforms in Eqs. (14) and (15) are not overlapped in time, then the joint probability density function for $\hat{\gamma}^2$ and $\hat{\psi}$ can be obtained from Ref. 12

$$p(\hat{\gamma}^2, \hat{\psi} \mid \gamma^2, \psi, N) = \frac{(1 - \gamma^2)^N}{2\pi\Gamma(N)\ \Gamma(N-1)} \ (1 - \hat{\gamma}^2)^{N-2} \sum_{k=0}^{\infty} \frac{2^k\ |\gamma|^k\ \Gamma^2(N + k/2)}{\Gamma\,(k + 1)}$$

$$(\hat{\gamma}^2)^{\frac{k}{2}} \cos\,(\hat{\psi} - \psi) \tag{16}$$

where Γ denotes a gamma function, γ^2 and ψ are the true values of MSC and cross-spectral phase, and N is the number of transforms used in estimating these parameters. It can also be shown that

$$P[\hat{\gamma}^2(w_k), \hat{\psi}(w_k), \hat{\gamma}^2(w_\ell), \hat{\psi}(w_\ell)] \approx P[\hat{\gamma}^2(w_k), \hat{\psi}(w_k)]\ P[\hat{\gamma}^2(w_\ell), \hat{\psi}(w_\ell)] \tag{17}$$

for any value of k not equal to ℓ. This follows from the fact that both $[F(w_k, n), F(w_\ell, n)]$ and $[H(w_k, n), H(w_\ell, n)]$ are asymptotically independent (Refs. 13, 14, 15) for $k \neq \ell$. Equations (16) and (17) provide the foundation for determining the statistics of the low-coherence forms of Λ_{GLR} and Λ_{AML}. However, even with this foundation, development of analytical expressions for P_{FA} and P_D which are algebraically tractable (i.e., in a convenient form to use and numerically well-conditioned) is difficult. Consequently, asymptotic

---

[12] N. Goodman, "On the Joint Estimation of the Spectra, Cospectrum, and Quadrature Spectrum of a Two-Dimensional Stationary Gaussian Process," Scientific Paper No. 10, Engineering Statistics Laboratory, New York University, March 1957.

[13] V. MacDonald and P. Schultheiss, "Optimum Passive Bearing Estimation in a Spatially Incoherent Noise Environment," *J. Acoust. Soc. Am.*, vol. 37, pp. 37-43, December 1968.

[14] W. Hodgkiss and L. Nolte, "Covariance Between Fourier Coefficients Representing the Time Waveforms Observed From an Array of Sensors," *J. Acoust. Soc. Am.*, vol. 59, pp. 582-590, March 1976.

[15] M. Rosenblatt, *Random Processes*, Springer-Verlag, 1962.

series solutions for both P_{FA} and P_D will be developed. The asymptotic series provide accurate expressions for P_{FA} and P_D, provided the parameter "N" in Eqs. (14) and (15) is large. Details of the derivation of the series are left for the appendices. Here, the general technique employed, the resulting expression, and limitations upon use of the expression will be discussed.

PROBABILITY OF FALSE ALARM

The probability of false alarm expression is derived under condition of noise only present. Under this condition, Eq. (16) reduces to

$$P(\hat{\gamma}^2, \hat{\psi} \mid \gamma^2=0, \psi, N) = \frac{N-1}{2\pi}(1-\hat{\gamma}^2)^{N-2}, \tag{18}$$

which shows that the sampled values of MSC and the cross-spectral phase are statistically independent. The density function of Eq. (18) can be used to derive the characteristic function of $\hat{\gamma}^2\cos\hat{\psi}$ and $\hat{\gamma}^2\cos^2\hat{\psi}$ by one of several techniques (Ref. 16). Denoting these characteristic functions as $g_{AML}(U)$ and $g_{GLR}(U)$, respectively, the probability density of Λ_{GLR} and Λ_{AML} can be evaluated as

$$P(\Lambda_{AML} \mid \gamma^2 = 0, N, M) = \frac{1}{2\pi}\int_{-\infty}^{\infty} [g_{AML}(u)]^m e^{iu\Lambda_{AML}}\, du \tag{19}$$

$$P(\Lambda_{GLR} \mid \gamma^2 = 0, N, M) = \frac{1}{2\pi}\int_{-\infty}^{\infty} [g_{GLR}(u)]^m e^{iu\Lambda_{GLR}}\, du \tag{20}$$

where M is the number of frequency regions or summation terms in the likelihood expressions. Integrating the density functions between a specified threshold, T, and infinity provides P_{FA} as a function of T. The details of these calculations are contained in Appendix B and lead to the asymptotic series solutions*

Generalized Likelihood Ratio $\Rightarrow$

$$P_{FA}(T) = \left[\frac{2^N(N-1)!}{(1;2;N-1)}\frac{1}{\sqrt{\pi}}\right]^M \left[(N-1.5)^{\frac{M}{2}}\left(\frac{N}{2}-1\right)!\right]^{-1}$$
$$\left[\Gamma\left(\frac{M}{2}, NT-1.5T\right) - \frac{1.5}{(N-1.5)(M+2)}\right.$$
$$\left.\Gamma\left(\frac{M}{2}+2, NT-1.5T\right) + \ldots\right] \tag{21}$$

---

[16] A. Papoulis, *Probability, Random Variables, and Stochastic Processes*, McGraw-Hill, 1965.

*The expressions presented here are applicable only when M is an even integer. Expressions for cases of M as an odd integer can be obtained from Appendix B.

$$\begin{array}{l}\text{Approximated} \\ \text{Maximum Likelihood}\end{array} \Rightarrow P_{FA}(T) = \frac{(N-1)^M}{(2N-4)^{(M-1)/2}\Gamma\left(\frac{M}{2}\right)} \left[\sum_{k=0}^{(M/2)-1} \frac{\left(\frac{M}{2}-1+k\right)!}{k!\left(\frac{M}{2}-1-k\right)!} \right.$$

$$\frac{2^{-(k+1/2)}}{(N-2)^{\frac{M-1}{2}}} \Gamma\left(\frac{M}{2}-k, NT-2T\right) + \frac{1}{2}\sum_{k=0}^{M/2} \frac{\left(\frac{M}{2}+k\right)!}{k!\left(\frac{M}{2}-k\right)!}$$

$$\left. \frac{2^{-(k+1/2)}}{(N-2)^{\frac{M+3}{2}}} \Gamma\left(\frac{M}{2}-k+1, NT-2T\right) - \ldots \right] \quad (22)$$

where $\Gamma(,)$ denotes an incomplete gamma function and $(a;b;c)$ denotes $a(a+b)(a+2b)\ldots(a+cb-b)$. No simulations have been conducted to verify the range of parameters over which the asymptotic series results are valid. It will be stated only that the series expressions increase in accuracy as N increases and that breakdown of the series can be expected when the higher order correction terms become as large as the leading order terms in an absolute value sense.

Plots of P_{FA} as a function of the specified threshold are presented in Fig. 1 for M=4 and N=64. Similarly, in Fig. 2 plots of P_{FA} versus threshold are presented for M=4 and N=128. The low-coherence form of Λ_{GLR} requires a slightly larger threshold than Λ_{AML}. This is reasonable in that both algorithms have very similar forms for low input coherence except for the non-zero mean of Λ_{GLR}. Both P_{FA} expressions are also nearly exponential in nature for N large.

PROBABILITY OF DETECTION

Probabilities of detection for the two likelihood-based algorithms can be evaluated using the same techniques as for P_{FA}, except starting with Eq. (16) instead of Eq. (18). The same degree of accuracy in the resulting expressions need not be required though. The P_{FA} expression depends upon the extreme tail of the density functions such that very careful approximations are required. P_D depends upon the bulk of the density function (if P_D's in the range of 0.1 to 0.9 are primarily of interest) such that coarser approximations can be made. The fact that a coarser approximation can be made and the fact that the signal-plus-noise density functions are more difficult to handle analytically motivates use of a classical approximation technique such as an Edgeworth series (Ref. 9). An Edgeworth series is an asymptotic series based upon a normal distribution and its derivatives. Functionally, the series provides the probability density function for a sum of independent random variables in terms of the moments of the individual random variables. Therefore, knowledge of the moments of $\gamma^2\cos\psi_k$ and $\gamma^2\cos^2\psi_k$ can be used to directly determine the probability density function of Λ_{GLR} and Λ_{AML} with signal plus noise being present. Integrating the resulting density functions between a specified threshold, T, and ∞ provides the probability of detection as a function of T.

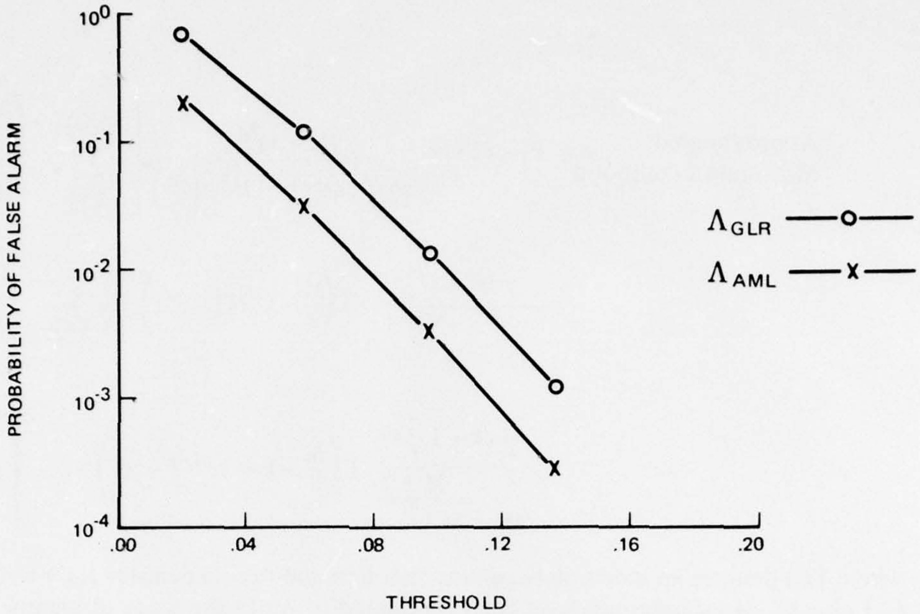

Figure 1. Probability of false alarm as a function of threshold for the likelihood expressions; N=64, M=4.

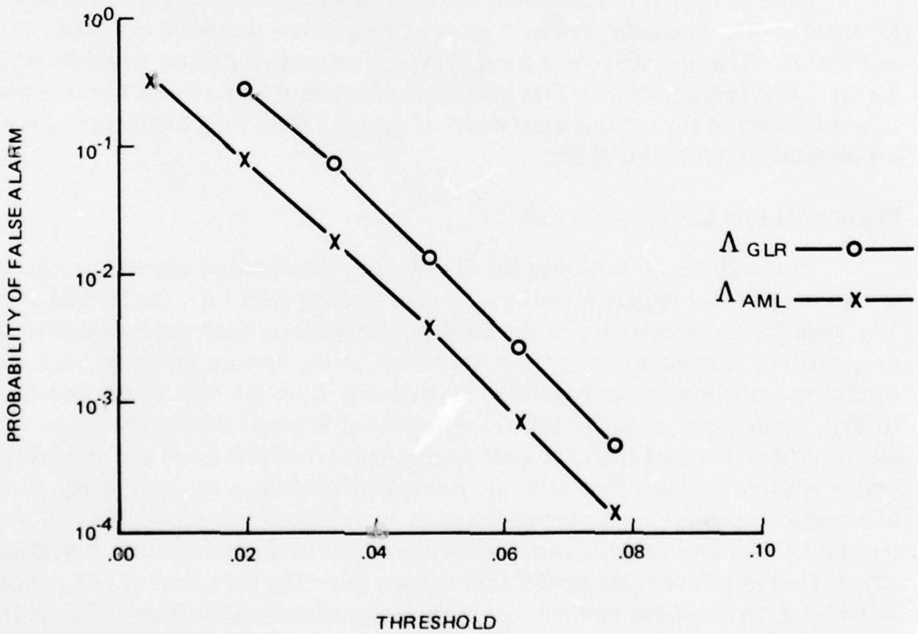

Figure 2. Probability of false alarm as a function of threshold for the likelihood expressions; N=128, M=4.

Details on the derivation and convergence properties of an Edgeworth series can be found in Refs. 2 and 9. Here, only the resulting expression for P_D will be presented

$$P_D(T) \sim \mathrm{erfc}\,(z) + \frac{C_1}{6}\,\phi^{(2)}(z) - \frac{C_2}{24}\,\phi^{(3)}(z) - \frac{C_1^2}{72}\,\phi^{(5)}(z) + \ldots, \tag{23}$$

$$z = \frac{T - \mu}{\sigma},$$

where $\phi^{(n)}$ denotes the n^{th} derivative of a normal density function, T denotes the selected threshold, C_n denotes the n^{th} cumulant, μ the mean, and σ the standard deviation, each of which are for the M summed random variables defined in Eqs. (8) and (9). Specification of C_n, μ, and σ in terms of the moments of the input random variables can be found in Chapter 26 of Ref. 17. Similarly, specification of $\phi^{(n)}$ in terms of Hermite polynomials can be found in Chapter 12 of Ref. 9. The only quantities necessary to implement Eq. (23) are the moments of $\hat{\gamma}^2\cos\hat{\psi}$ and $\hat{\gamma}^2\cos^2\hat{\psi}$. These moments can be computed directly from Eq. (16) as

Generalized Likelihood Ratio Expression:

$$\mu'_m = \int_{-\infty}^{\infty}\int_{-\infty}^{\infty}\left[\hat{\gamma}^2\cos^2\hat{\psi}\right]^m p\left(\hat{\gamma}^2, \hat{\psi}\,|\,\gamma^2, \psi, N\right) d\hat{\gamma}\, d\hat{\psi} \tag{24}$$

$$= \frac{(1-\gamma^2)}{\Gamma(N)\,\Gamma(N-1)} \sum_{k=0}^{\infty} \frac{2^{k-1}\Gamma^2(N + k/2)\,\Gamma\left(\frac{k}{2} + m + \frac{1}{2}\right)}{\Gamma(k+1)\,\Gamma\left(\frac{k}{2} + m + 1\right)} (\gamma^2)^{k/2}$$

$$\frac{\Gamma(N-1)\left[1 + (-1)^{k+2m}\right]}{\left(m + \frac{k}{2} + 1; 1; N-1\right)} \tag{25}$$

Approximated Maximum Likelihood Expression:

$$\mu'_m = \int_{-\infty}^{\infty}\int_{-\infty}^{\infty}\left[\hat{\gamma}^2\cos\hat{\psi}\right]^m p\left(\hat{\gamma}^2, \hat{\psi}\,|\,\gamma^2, \psi, N\right) d\hat{\gamma}^2\, d\hat{\psi} \tag{26}$$

$$= \frac{(1-\gamma^2)^{N-2}}{\Gamma(N)\,\Gamma(N-1)} \sum_{k=0}^{\infty} \frac{2^{k-1}\,\Gamma^2\left(N + \frac{k}{2}\right)\Gamma\left(\frac{k}{2} + \frac{m}{2} + \frac{1}{2}\right)}{\Gamma(k+1)\,\Gamma\left(\frac{k}{2} + \frac{m}{2} + 1\right)} (\gamma^2)^{k/2}$$

$$\frac{\Gamma(N-1)\left[1 + (-1)^{k+m}\right]}{\left(m + \frac{k}{2} + 1; 1; N-1\right)} \tag{27}$$

---

[17] M. Abramowitz and I. Stegun, "Handbook of Mathematical Functions," National Bureau of Standards, Applied Mathematic Series 55, June 1964.

where μ'_m denotes the m^{th} moment centered about the origin.

Equations (23) through (27) can be utilized to determine the detection performance of the low-coherence forms of Λ_{GLR} and Λ_{AML}. Use of Eqs. (21) and (22) allow the detection performances to be evaluated on the basis of a specified P_{FA}. As a first illustration, the probability of detections for Λ_{GLR}, Λ_{AML}, and a normalized cross-correlation will be compared for the situation of flat signal and noise spectral properties across the input bandpass. The probabilities of detection and false alarm for a normalized cross-correlation can be calculated from Eqs. (29.7.1) through (29.7.5) of Ref. 9. The parameters selected for the comparison are N=64, M=4, and $P_{FA}=10^{-3}$ for the likelihood expressions, which represents an equivalent number of degrees of freedom for the normalized cross-correlation processor of 512. In Fig. 3, the probabilities of detection as a function of input signal-to-noise ratio are presented for all three algorithms. The normalized cross correlation processor shows an improvement of 0.2 and 1.0 dB, respectively, over Λ_{AML} and Λ_{GLR}. This result is not surprising, the likelihood expressions are formulated for cases where the spectral properties vary across the input bandpass and should not be expected to provide processing gain over a normalized cross-correlation processor whose processing bandwidth is matched to the signal bandwidth.*

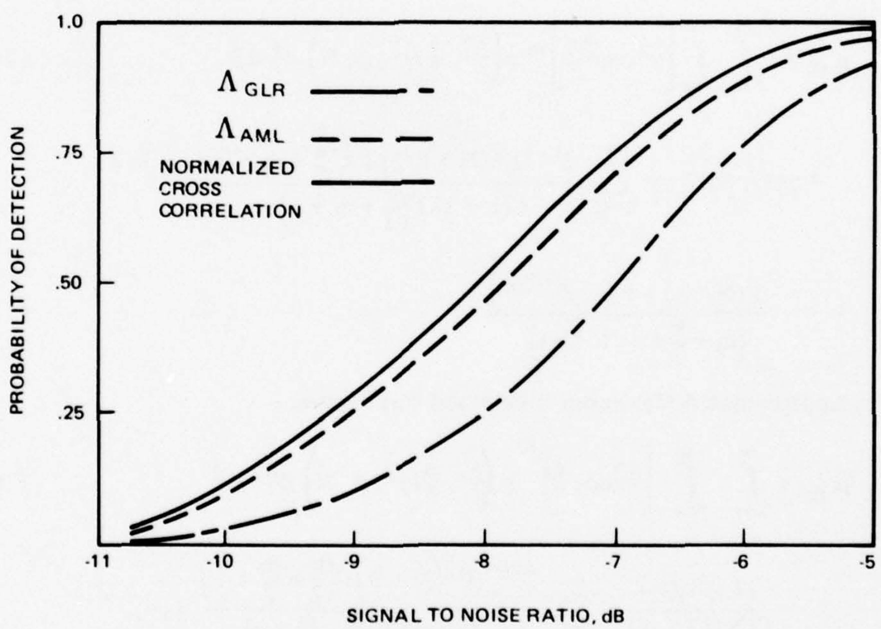

Figure 3. Probability of detection as a function of input signal to noise ratip; P_{FA} = 10^{-3}, flat input signal and noise spectra, 512 degrees of freedom.

*For flat spectral characteristics, the likelihood expressions can be expected to provide degraded performance relative to a normalized cross-correlation processor as the value M is increased. A simple proof of this is presented in Appendix C.

The primary benefit from the likelihood expressions will occur when the signal or noise spectral levels vary as a function of frequency across the input bandpass. Under this condition, the coherence weights estimated in each frequency interval will adapt to the varying spectral properties. Improvement over a normalized cross-correlation can be illustrated for the case of the processing bandwidth being wider than the signal bandwidth. A mismatched processing bandwidth is depicted in Fig. 4. The noise spectral density is N over the input processing bandwidth, B_p. The signal spectral density is S over the region B_s, where B_s is less than B_p. For comparison purposes between Λ_{AML} and a normalized cross-correlation, let P_{FA} for each algorithm be set at 10^{-3}, let Λ_{AML} estimate coherence weights in frequency regions of width B_s, and let the coherence weights be estimated with 64 transform values (i.e., the time-bandwidth product for both processors is 64 B_p/B_s). In Fig. 5, the ratio of S/N necessary to achieve a P_D of 0.5 is plotted as a function of the bandwidth mismatch, B_p/B_s. Both processors require nearly the same ratio of S/N with no mismatch. But as the mismatch increases, the normalized cross-correlation requires vaues of S/N that grow at a faster rate. The normalized cross-correlation requires a value of S/N that increases by approximately 1.5 dB every time the value of B_p/B_s doubles. The likelihood expression requires a value of S/N that increased by approximately .75 dB every time the value of B_p/B_s doubles. That is, the likelihood expression is less subject to performance degradation due to processing mismatch than a normalized cross-correlation. This same conclusion can be drawn from examining the deflection ratios of each algorithm (ratio of mean output with signal present to the standard deviation with noise only present) as is shown in Appendix C.

Additional examples of processing gain for the likelihood expressions can be illustrated for the case of colored noise or interference across the input processing bandpass. Processing gain in these situations can easily be expected because the likelihood expressions do not depend upon absolute spectral levels as a function of frequency but only upon the measured coherence as a function of frequency. Here, an example involving colored noise will be demonstrated through the use of an ambiguity surface calculation. The expectation values of the cross-spectral properties selected for the example are presented in Fig. 6. The noise power falls linearly over the input processing bandpass. A narrowband signal is situated in the center of the bandpass and possesses a level corresponding to a –14-dB signal-to-noise ratio relative to the 12-Hz processing bandpass. A single realization of these cross-spectral properties was created and processed through the Λ_{AML} algorithm and a normalized cross-correlation.* The Λ_{AML} algorithm estimated coherence weights in 1-Hz regions across the 12-Hz processing bandpass. In Figs. 7 and 8, ambiguity surfaces resulting from each algorithm are presented. Height of the data in the ambiguity surface is color encoded, with the highest data point in each surface represented by the color red. The dimensions of the ambiguity surface are time-difference and Doppler difference between the two input time series. The position of these parameters for the synthetic signal is denoted by the black arrows in Fig. 7. The ambiguity surface created with the Λ_{AML} algorithm shows the highest peak in the surface located at the synthetic signal's time and frequency difference parameters. For the normalized cross-correlation calculation, the peak corresponding to the signal's

*Envelope versions of each of these algorithms were utilized. The envelope of Λ_{AML} is defined by Eq. (13) and the envelope of a normalized cross-correlation corresponds to estimates of magnitude squared coherence.

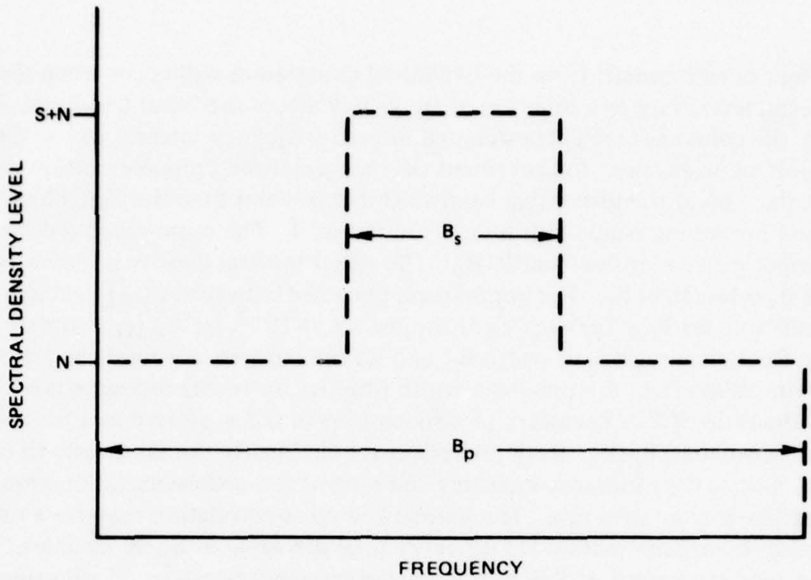

Figure 4. Depiction of processing mismatch to the signal bandwidth. Signal possesses a bandwidth of B_s and a spectral density of *S*. Processing bandpass is B_p with a noise spectral density of *N*.

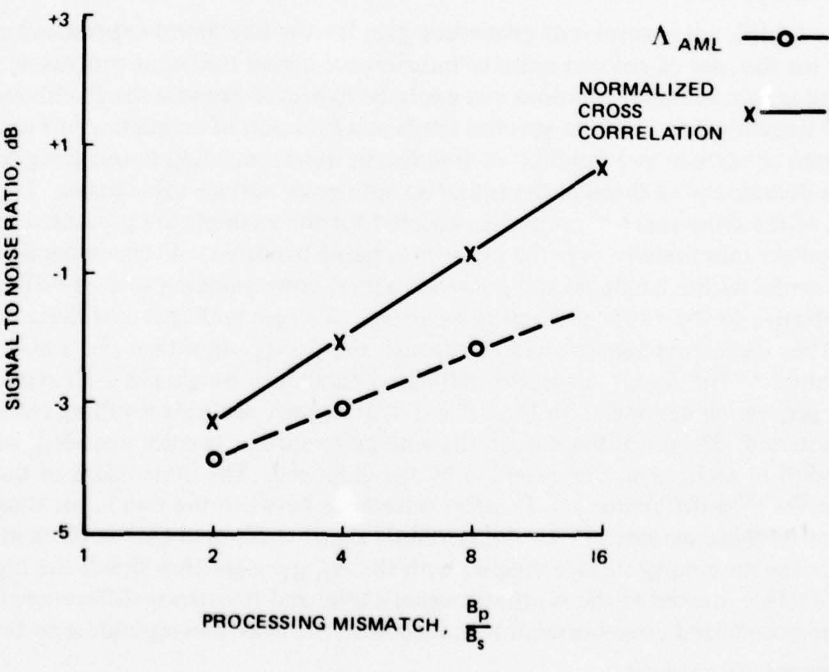

Figure 5. Signal to noise ratio necessary to obtain a probability of detection of 0.5 as a function of the mismatch of processing bandpass to signal bandpass; $P_{FA} = 10^{-3}$.

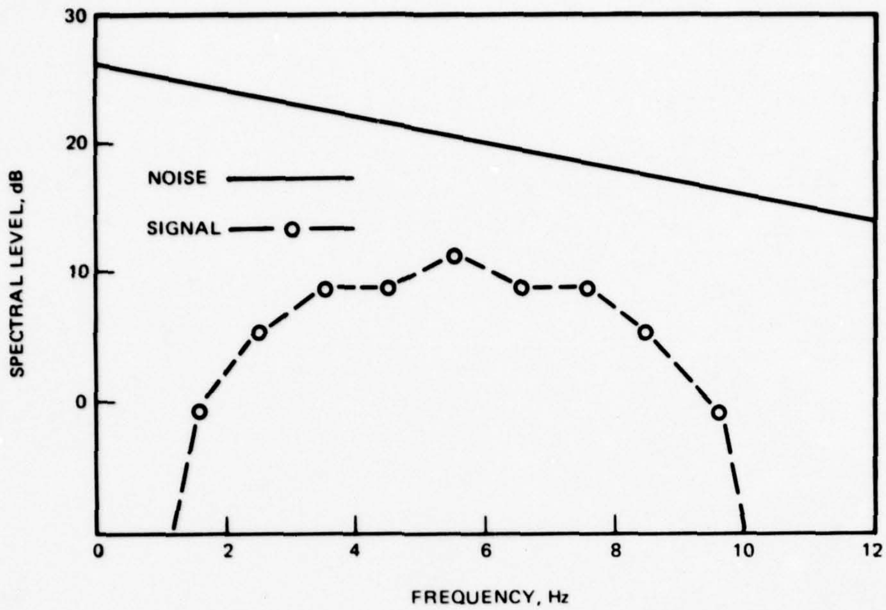

Figure 6. Signal and noise cross spectral properties for the synthetic data.

parameters is smaller than two noise spikes on the surface. The data in Fig. 7 was created with a total time-bandwidth product into each algorithm of 1800. If the time-bandwidth product is decreased to 1200, the ambiguity surfaces presented in Fig. 8 result. The signal peak has now essentially disappeared from the surface resulting from the normalized cross-correlation. For the surface generated with Λ_{AML}, the largest peak on the surface still corresponds to the time and frequency difference of the synthetic signal.

4.0 CONCLUSION

In this report, we have demonstrated that likelihood-based filtering of the cross-spectrum can provide improved detection and parameter estimation performance over that of a normalized cross-correlation processor. The improvement will occur when the signal and noise spectral properties vary over the input bandpass. Such a situation can be expected when little *a priori* information exists about the signal properties or if the noise background is highly variable, conditions which do occur in low-frequency acoustic processing. Therefore, the likelihood expressions represent a viable technique for conducting joint detection and parameter estimation on the output of two sensors.

Demonstrations of processing performance with the two likelihood expressions examined were presented analytically in the form of Receiver Operating Characteristics and graphically with processing results on synthetic data. No major differences in the performance between the two algorithms were observed. It is felt that major differences between the generalized likelihood ratio expression and the constrained maximum likelihood expression will only occur in the parameter estimation capability for wideband signals. Analytical determination of these differences may be quite difficult such that the performance comparison should be conducted empirically.

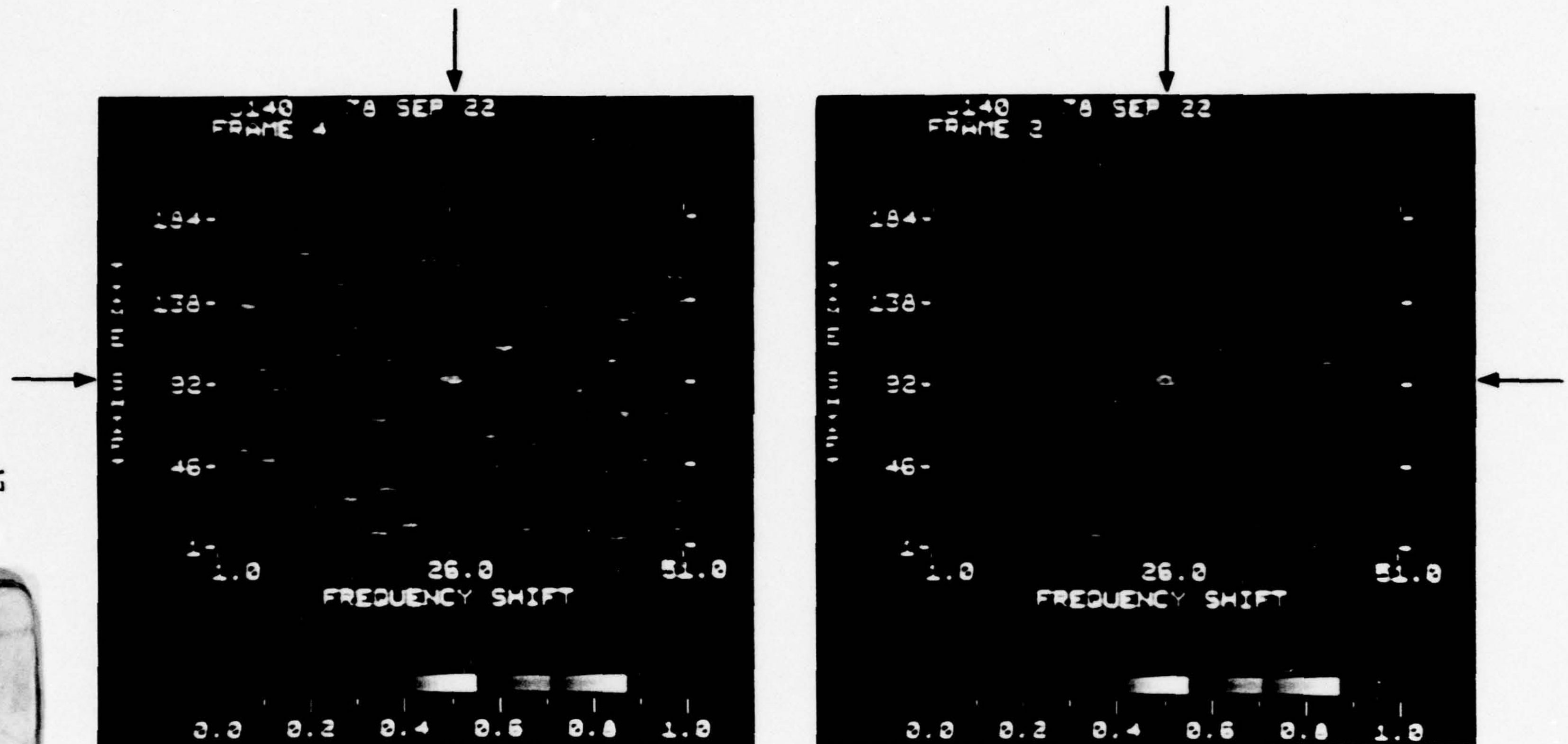

APPROXIMATED MAXIMUM LIKELIHOOD

NORMALIZED CROSS CORRELATION

Figure 7. Comparative ambiguity surfaces showing improvement of likelihood ratio technique over a normalized cross correlation, time-bandwidth product of 1800.

PRECEDING PAGE BLANK-NOT FILMED

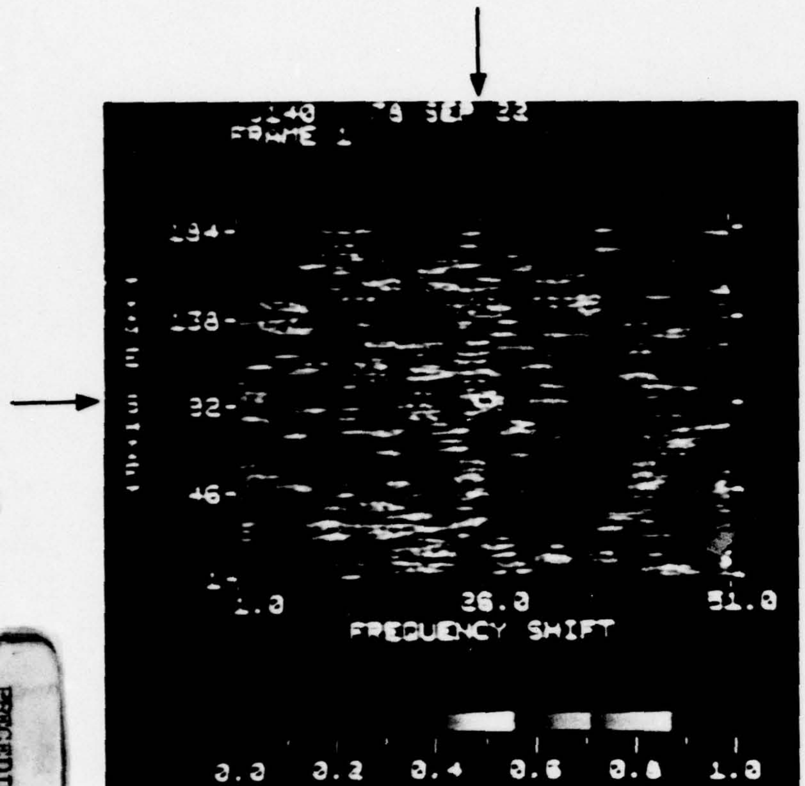

APPROXIMATED MAXIMUM LIKELIHOOD

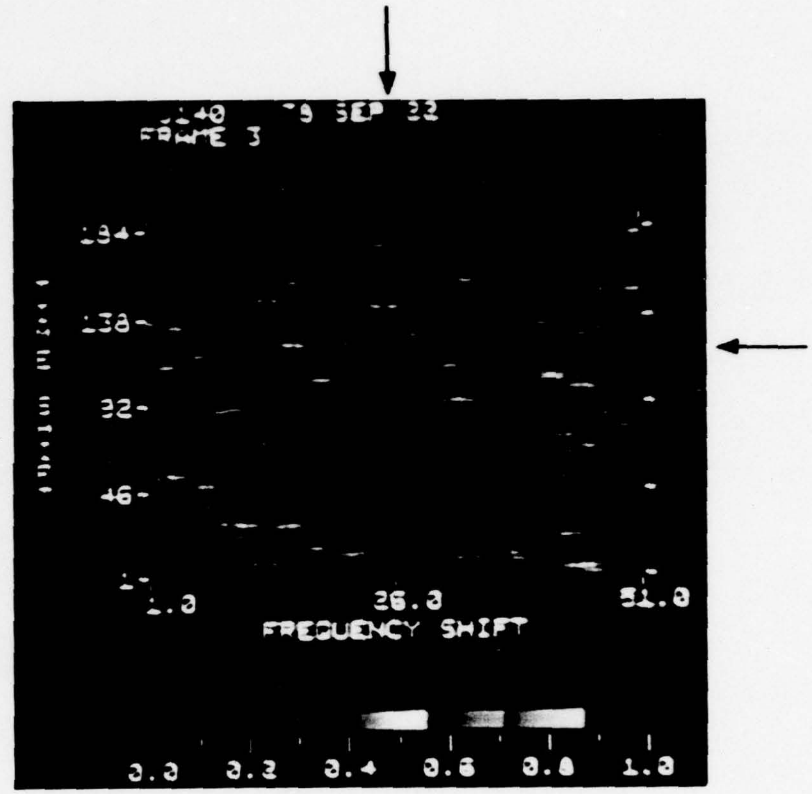

NORMALIZED CROSS CORRELATION

Figure 8. Comparative ambiguity surfaces showing improvement of likelihood ratio technique over a normalized cross correlation, time-bandwidth product of 1200.

PRECEDING PAGE BLANK-NOT FILMED

Finally, improvements upon the cross-spectral filtering approaches presented in this report may be easily realized. The adaptations analyzed here were single-step in nature. If the signal and noise characteristics remain stationary over time periods longer than a single observation, the coherence estimates as a function of frequency can be smoothed recursively in time. The performance of the likelihood expressions can also be improved by a judicious choice of the number of frequency regions that coherence weights are estimated in across the processing bandpass. This selection will be dependent upon coarse information concerning signal and noise properties for the case of interest.

REFERENCES

1. W.J. Bangs, "Array Processing With Generalized Beam-Formers," Ph.D. Dissertation, Yale University, New Haven, Connecticut, September 1971.
2. C.W. Helstrom, *Statistical Theory of Signal Detection*, Permagon Press, 1968.
3. H.L. Van Trees, *Detection, Estimation, and Modulation Theory, Part I*, John Wiley and Sons, 1968.
4. D. Middleton, *An Introduction to Statistical Communication Theory*, McGraw-Hill, 1960.
5. T. Arase and E. Arase, "Deep Sea Ambient Noise Statistics," *J. Acoust. Soc. Am.*, Vol. 44, pp. 1679-1684, April 1968.
6. D. Becker, "Investigate the Use of Alternate Sample Statistics," ORINCON Company Report, prepared under Contract N000123-76-C-0505, December 1976.
7. Reference available to qualified requesters.
8. P.M. Schultheiss, "Estimation of Doppler Shift and Differential Doppler Shift," Yale University, Technical Report, prepared under Contract N66001-76-C-1082, June 1977.
9. H. Cramer, *Mathematical Methods of Statistics*, Princeton University Press, 1946.
10. G. Carter, "Time Delay Estimation," NUSC TR 5335, April 1976.
11. E. Hannan and J. Thompson, "Estimating Group Delay," *Biometrika*, Vol. 60, pp. 241-253, 1973.
12. N. Goodman, "On the Joint Estimation of the Spectra, Cospectrum, and Quadrature Spectrum of a Two-Dimensional Stationary Gaussian Process," Scientific Paper No. 10, Engineering Statistics Laboratory, New York University, March 1957.
13. V. MacDonald and P. Schultheiss, "Optimum Passive Bearing Estimation in a Spatially Incoherent Noise Environment," *J. Acoust. Soc. Am.*, Vol. 37, pp. 37-43, December 1968.
14. W. Hodgkiss and L. Nolte, "Covariance Between Fourier Coefficients Representing the Time Waveforms Observed From an Array of Sensors," *J. Acoust. Soc. Am.*, Vol. 59, pp. 582-590, March 1976.
15. M. Rosenblatt, *Random Processes*, Springer-Verlag, 1962.

PRECEDING PAGE BLANK-NOT FILMED

16. A. Papoulis, *Probability, Random Variables, and Stochastic Processes*, McGraw-Hill, 1965.

17. M. Abramowitz and I. Stegun, "Handbook of Mathematical Functions," National Bureau of Standards, Applied Mathematic Series 55, June 1964.

18. G. Carter, "Estimation of the Magnitude-Squared Coherence Function," NUSC TR 4343, May 1972.

19. R. Merk and S. McCarthy, "Statistics of Averaged Mangitude Squared Coherence," CMAP Research Report No. 77-014, Naval Ocean Systems Center, April 1978.

20. I. Gradshteyn and I. Ryzhik, *Tables of Integral Series and Products*, Academic Press, 1965.

21. W. Grobner and N. Hofreiter, *Integraltafel Erster Teil Unbestimmte Integrale, Integraltafel Zweiter Teil Bestimmte Integrale*, Springer-Verlag, 1966.

22. A. Erdely, *Tables of Integral Transforms, Volume I*, McGraw-Hill, 1954.

23. S. Shelby, "Standard Mathematical Tables," The Chemical Rubber Company, 1964.

APPENDIX A
GENERALIZED LIKELIHOOD RATIO TEST STATISTIC

The generalized likelihood ratio test statistic has the form (Refs. 3, 4, 6)

$$\Lambda_{GLR} = \frac{p(\bar{z}\,|\bar{\theta}_1)\,\{\text{max. over } \bar{\theta}_1\}}{p(\bar{z}\,|\bar{\theta}_0)\,\{\text{max. over } \bar{\theta}_0\}} \tag{A-1}$$

where $\bar{z}$ is the vector of observation data from two sensors, $p(\bar{z}|\bar{\theta})$ represents the conditional density of the input data on the parameter set $\bar{\theta}$, and $\bar{\theta}_1$ and $\bar{\theta}_0$ denote, respectively, the parameter sets under condition of signal plus noise and noise only being present. Without loss of generality, the vector of observation data can be comprised of the Fourier transform of the time series data from each sensor. Letting $\bar{z}$ denote the observation vector of complex Fourier components and constraining both the signal and noise to be realized from a Gaussian process, the probability density functions can be written as

$$p(\bar{z}|\Phi) = \pi^{-2m}\,|\Phi|^{-1}\exp\left\{-\bar{z}^{+}\,\Phi^{-1}\,\bar{z}\right\} \tag{A-2}$$

where m is the size of the vector of observation and Φ denotes the correlation matrix under the two different hypotheses. Provided the input spectra is well behaved, the above density function can be partitioned as (Refs. 10, 13, 14)

$$p(\bar{z}|\Phi) = \pi^{-2m}\prod_{k=1}^{\frac{m}{2}}\left|\Phi_k\right|^{-1}\exp\left\{-\bar{z}_k^{+}\,\Phi_k^{-1}\,\bar{z}_k\right\} \tag{A-3}$$

where $\bar{z}_k$ denotes the complex Fourier components for the k^{th} frequency region and Φ_k is the correlation matrix for the k^{th} frequency region (Φ_k is a two-by-two dimension). Under condition of signal plus noise being present, the partitioned correlation matrices have the form

$$\Phi_k = \begin{bmatrix}\sigma_{11}(k) & \sigma_{12}(k)\,e^{-iw_k\tau}\\ \sigma_{12}(k)\,e^{iw_k\tau} & \sigma_{22}(k)\end{bmatrix} \tag{A-4}$$

where $\sigma_{11}(k)$, $\sigma_{22}(k)$, and $\sigma_{12}(k)$ are the unknown auto and absolute cross-spectral levels for the k^{th} frequency region, and τ is the signal travel time difference between the sensors. Under condition of noise only being present, the partitioned correlation matrices have the form

$$\Phi_k = \begin{bmatrix}\sigma_{11}(k) & 0\\ 0 & \sigma_{22}(k)\end{bmatrix} \tag{A-5}$$

Equation (A-3) can also be expressed in the form

$$p(\bar{z}|\Phi) = \pi^{-2m}\prod_{k=1}^{\frac{m}{2}}\left|\Phi_k\right|^{-1}\exp\left[-\mathrm{Tr}\left(\chi_k\;\Phi_k^{-1}\right)\right] \tag{A-6}$$

where χ_k is defined as

$$\chi_k = \bar{z}_k \, \bar{z}_k^+ \qquad \text{(A-7)}$$

and represents the sampled correlation matrix for the k^{th} frequency region. If multiple observations in time are taken, the only change in form for Eq. (A-6) is that the sampled correlation matrix is now represented by the smoothed matrix

$$\chi_k = \sum_{\ell=1}^{L} \bar{z}_k(\ell) \, \bar{z}_k(\ell)^+ \qquad \text{(A-8)}$$

where $\bar{z}_k(\ell)$ denotes the Fourier components for the k^{th} frequency region and the ℓ^{th} time period, and π^{-2m} in equation (A-6) is replaced by π^{-2mL}. In order to generate Λ_{GLR}, Eq. (A-6) needs to be maximized for Φ_k of the form of Eq. (A-4) and then for Φ_k of the form of Eq. (A-5).

SIGNAL PLUS NOISE PRESENT

The numerator of Eq. (A-1) is obtained by solving the set of simultaneous equations

$$\frac{\partial}{\partial \sigma_{11}(k)} p(\bar{z}\,|\,\Phi) = \frac{\partial}{\partial \sigma_{22}(k)} p(\bar{z}\,|\,\Phi) = \frac{\partial}{\partial \sigma_{12}(k)} p(\bar{z}\,|\,\Phi) = \frac{\partial}{\partial \tau} p(\bar{z}\,|\,\Phi) = 0 \qquad \text{(A-9)}$$

for all values of k where the partitioned correlation matrices are of the form of Eq. (A-4). Differentiating Eq. (A-6) with respect to $\sigma_{11}(k)$, $\sigma_{22}(k)$, and $\sigma_{12}(k)$ leads to the three simultaneous equations

$$\mathrm{Tr}\left[\chi_k \Phi_k^{-1}\right] = 1 + \frac{\frac{\partial}{\partial \sigma_{11}(k)} \mathrm{Tr}\left(\chi_k \hat{\Phi}_k\right)}{\frac{\partial}{\partial \sigma_{11}(k)} |\Phi_k|} = 1 + \frac{x_{22}(k)}{\sigma_{22}(k)} \qquad \text{(A-10)}$$

$$\mathrm{Tr}\left(\chi_k \Phi_k^{-1}\right) = 1 + \frac{\frac{\partial}{\partial \sigma_{22}(k)} \mathrm{Tr}\left(\chi_k \hat{\Phi}_k\right)}{\frac{\partial}{\partial \sigma_{22}(k)} |\Phi|} = 1 + \frac{x_{11}(k)}{\sigma_{11}(k)} \qquad \text{(A-11)}$$

$$\mathrm{Tr}\left[\chi_k \Phi_k^{-1}\right] = 1 + \frac{\frac{\partial}{\partial \sigma_{12}(k)} \mathrm{Tr}\left(\chi_k \hat{\Phi}_k\right)}{\frac{\partial}{\partial \sigma_{12}(k)} |\Phi_k|} = 1 + \frac{R\ell\left[x_{12}(k)\, e^{-iw_k\tau}\right]}{\sigma_{12}(k)} \qquad \text{(A-12)}$$

where $\wedge$ denotes adjoint and the x terms are elements of χ_k. The simultaneous solutions for $\sigma_{11}(k)$, $\sigma_{22}(k)$, and $\sigma_{12}(k)$ defined by the above three equations are found through manipulation to be

$$\sigma_{11}(k) = x_{11}(k) \qquad \text{(A-13)}$$

$$\sigma_{22}(k) = x_{22}(k) \qquad \text{(A-14)}$$

$$\sigma_{12}(k) = R\ell \left[x_{12}(k)\ e^{-iw_k \tau} \right]. \qquad \text{(A-15)}$$

Substituting these solutions back into the numerator of Eq. (A-1) provides

$$p(\bar{z}|\bar{\theta}_1)\left(\text{max. over } \bar{\theta}_1\right) = \pi^{-2mL} \exp(-2L) \prod_{k=1}^{\frac{m}{2}} \Big\{ x_{11}(k)\, x_{22}(k) - R\ell^2 \left[x_{12}(k)\ e^{-iw_k \tau} \right] \Big\}^{-1} \left(\text{max. over } \tau\right). \qquad \text{(A-16)}$$

Although the maximization with respect to τ is easy to derive analytically, the form of Eq. (A-16) turns out to be more convenient for our purposes.

NOISE-ONLY PRESENT

The denominator of Eq. (A-1) is obtained by solving the set of simultaneous equations

$$\frac{\partial}{\partial \sigma_{11}(k)}\, p(\bar{z}|\Phi) = \frac{\partial}{\partial \sigma_{22}(k)}\, p(\bar{z}|\Phi) = 0 \qquad \text{(A-17)}$$

for all values of k where the partitioned correlation matrices are of the form of Eq. (A-5). The form of these solutions is the same as Eqs. (A-10) and (A-11) but with Φ_k defined by Eq. (A-5). The solution to these simultaneous equations is simply given by

$$\sigma_{11}(k) = x_{11}(k) \qquad \text{(A-18)}$$

$$\sigma_{22}(k) = x_{22}(k) \qquad \text{(A-19)}$$

Substituting these solutions back into the denominator of Eq. (A-1) provides

$$p(\bar{z}|\bar{\theta}_0)\left(\text{max over } \bar{\theta}_0\right) = \pi^{-2mL} \exp\left(-2L\right) \prod_{k=1}^{\frac{m}{2}} \left[x_{11}(k)\, x_{22}(k) \right]^{-1}. \qquad \text{(A-20)}$$

GENERALIZED LIKELIHOOD RATIO

Equations (A-16) and (A-20) can be combined to form the likelihood ratio test statistic

$$\Lambda_{GLR} = \prod_{k=1}^{\frac{m}{2}} \left[\frac{x_{11}(k)\, x_{22}(k)}{x_{11}(k)\, x_{22}(k) - R\ell^2 \left(x_{12}(k)\, e^{-iw_k \tau} \right)} \right] \left(\text{max. over } \tau\right). \qquad \text{(A-21)}$$

Expressing $x_{12(k)}$ explicitly in terms of its real and imaginary components,

$$x_{12(k)} = |x_{12(k)}| \, e^{i\psi_k} \tag{A-22}$$

allows the likelihood ratio to be expressed as

$$= \prod_{k=1}^{\frac{m}{2}} \left[1 - \frac{x_{12}^{\;2}}{x_{11(k)}\, x_{22(k)}} \cos^2\left(\psi_k - w_k \tau\right) \right]^{-1} \quad \left(\text{max. over } \tau\right) \tag{A-23}$$

$$= \prod_{k=1}^{\frac{m}{2}} \left[1 - \hat{\gamma}^2_{(k)} \cos^2\left(\psi_k - w_k \tau\right)^{-1} \right] \left(\text{max. over } \tau\right) \tag{A-24}$$

where $\hat{\gamma}^2_{(k)}$ is the sampled magnitude squared coherence between the two sensors at radian frequency w_k. The log likelihood ratio is monotonic with respect to the above expression such that an equivalent test statistic is given by

$$\Lambda_{GLR} = - \sum_{w_k} \ln \left[1 - \hat{\gamma}^2_{(w_k)} \cos^2\left(\psi_k - w_k \tau\right) \right] \left(\text{max. over } \tau\right). \tag{A-25}$$

APPENDIX B
PROBABILITY OF FALSE ALARM EXPRESSIONS

Derivation of the probability of false alarm for the low level coherence forms of Λ_{GLR} and Λ_{AML} mainly involves evaluating integrals and Fourier transforms. These operations can be found for the most part in standard references. Here, steps available from standard references will be denoted by the reference number and the corresponding equation, both in square brackets.

APPROXIMATE MAXIMUM LIKELIHOOD

The noise-only density function for

$$\Lambda_{AML} = \sum_{k=1}^{M} \hat{\gamma}_k^2 \cos \hat{\theta}_k = \sum_{k=1}^{M} \hat{z}_k \quad ; \quad \hat{z}_k = \hat{\gamma}_k^2 \cos \hat{\theta}_k \tag{B-1}$$

can be obtained by calculating the characteristic function of $\hat{z}_k$, raising the characteristic function to the M^{th} power, and then inverting it. The characteristic function of $\hat{z}_k$ is defined by

$$g(u) = \int_{-\infty}^{\infty} e^{iu\hat{z}_k} \, \rho(\hat{z}_k) \, d\hat{z}_k \tag{B-2}$$

where $\rho(\hat{z}_k)$ denotes the probability density function of $\hat{z}_k$. The characteristic function can also be evaluated as (remembering that $\hat{\gamma}^2{}_k$ and $\hat{\theta}_k$ are statistically independent for noise only present)

$$g(u) = \int_{-\infty}^{\infty} \int_{-\infty}^{\infty} e^{iu\hat{\gamma}_k^2 \cos \hat{\theta}_k} \, \rho(\hat{\gamma}_k^2) \, \rho(\cos \hat{\theta}_k) \, d\hat{\gamma}_k^2 \, d \cos \hat{\theta}_k \tag{B-3}$$

$$= \int_{-\infty}^{\infty} \int_{-\infty}^{\infty} e^{iuxy} \, \rho(x) \, \rho(y) \, dx \, dy \quad ; \quad x=\hat{\gamma}_k^2 \text{ and } y=\cos \hat{\theta}_k . \tag{B-4}$$

The density functions for x and y are available from [16; 4.5] and [18; 5-15] such that

$$g(u) = \frac{N-1}{\pi} \int_{-1}^{1} \int_{0}^{1} e^{iuxy} \, (1-x)^{N-2} \, (1-y^2)^{-1/2} \, dx \, dy \tag{B-5}$$

where N is the number of transforms utilized in estimating $\hat{\gamma}_k^2$ and $\hat{\theta}_k$. The term $(1-x)^{N-2}$ can be written as

---

[18] G. Carter, "Estimation of the Magnitude-Squared Coherence Function," NUSC TR 4343, May 1972.

$$(1-x)^{N-2} = \exp\left[-(N-2)\sum_{\ell=1}^{\infty}\frac{x^\ell}{\ell}\right]. \qquad \text{(B-6)}$$

Substituting this series expression in Eq. (B-5) and making the change of variables B=N-2-iuy and r=xB leads to

$$g(u) = i\,\frac{N-1}{\pi}\int_{N-2+iu}^{N-2-iu}\int_0^B \exp\left\{-r-(N-2)\sum_{\ell=2}^{\infty}\frac{r^\ell}{\ell B^\ell}\right\}\left[u^2+(B-N+2)^2\right]^{-1/2}$$

$$\frac{1}{B}\,dr\;dB \qquad \text{(B-7)}$$

$$= i\,\frac{N-1}{\pi}\int_{N-2+iu}^{N-2-iu}\int_0^B e^{-r}\left[\frac{1}{B}-\frac{(N-2)r^2}{2B^3}-\frac{(N-2)r^3}{3B^4}+\ldots\right]$$

$$\left[u^2+(B-N+2)^2\right]^{-1/2}\,dr\,dB. \qquad \text{(B-8)}$$

In going from Eq. (B-7) to (B-8), the exponent terms for $\ell \geq 2$ have been rewritten in individual Taylor series expansions. The approximation that will be employed for g(u) is to change the upper limit on the integration with respect to r such that

$$g(u) \approx i\,\frac{N-1}{\pi}\int_{N-2+iu}^{N-2-iu}\int_0^\infty e^{-r}\left[\frac{1}{B}-\frac{(N-2)r^2}{2B^3}-\frac{(N-2)r^3}{3B^4}+\ldots\right]$$

$$\left[u^2+(B-N+2)^2\right]^{-1/2}\,dr\,dB. \qquad \text{(B-9)}$$

This approximation has been discussed in [19;16] and has been shown to be very accurate for N large. Carrying out the integration with respect to r provides

$$g(u) \approx i\,\frac{N-1}{\pi}\int_{N-2+iu}^{N-2-iu}\left[\frac{1}{B}-\frac{N-2}{B^3}-\frac{2(N-2)}{B^4}+\ldots\right]\left[u^2+(B-N+2)^2\right]^{-1/2} dB, \qquad \text{(B-10)}$$

where terms in the first bracket are ordered by their significance (remembering that N is restricted to be large and that $|B| > N-2$). The integration with respect to B can be carried out through the use of [20; 2.261, 2.266, 2.269] and [21; 231.9a] to provide

[19] R. Merk and S. McCarthy, "Statistics of Averaged Magnitude Squared Coherence," CMAP Research Report No. 77-014, Naval Ocean Systems Center, April 1978.

[20] I. Gradshteyn and I. Ryzhik, *Tables of Integral Series and Products*, Academic Press, 1965.

[21] W. Grobner and N. Hofreiter, *Integraltafel Erster Teil Unbestimmte Integrale, Integraltafel Zweiter Teil Bestimmte Integrale*, Springer-Verlag, 1966.

$$g(u) \approx \frac{N-1}{\left[u^2 + (N-2)^2\right]^{1/2}} + \frac{1}{2}\,\frac{(N-1)\,(N-2)}{\left[u^2 + (N-2)^2\right]^{3/2}} - \frac{3}{2}\,\frac{(N-1)\,(N-2)^3}{\left[u^2 + (N-2)^2\right]^{5/2}} + \dots \qquad \textbf{(B-11)}$$

Raising g(u) to the M^{th} power and ordering terms by their significance leads to

$$g^M_{(u)} \approx \frac{(N-1)^M}{\left[u^2 + (N-2)^2\right]^{M/2}} \left\{ 1 + \frac{M}{2}(N-2)\;\; u^2 + (N-2)^2 \;\; ^{-1} \; - \frac{3}{2} M \, (N-2) \right.$$

$$\left. \left[u^2 + (N-2)^2\right]^{-2} + \dots \right\} . \qquad \textbf{(B-12)}$$

The above characteristic function can be inverted through the use of [22; 1.3(7)] to provide the noise only density function for Λ_{ALR} of

$$\rho(\Lambda \,|\, M, N, \gamma^2{=}0) \approx \frac{(N-1)^M}{\sqrt{\pi}} \left\{ \frac{|\Lambda|^{(M-1)/2} \, K_{(M-1)/2}\,(N|\Lambda| - 2|\Lambda|)}{(2N-4)^{(M-1)/2}\;\Gamma\!\left(\frac{M}{2}\right)} + \frac{M}{2}\,(N-2) \right.$$

$$\left. \frac{|\Lambda|^{(M+1)/2} \, K_{(M+1)/2}\,(N|\Lambda| - 2|\Lambda|)}{(2N-4)^{(M+1)/2}\;\Gamma\!\left(\frac{M}{2} + 1\right)} - \dots \right\} \qquad \textbf{(B-13)}$$

where K denotes a modified Bessel function of the second kind and Γ denotes a gamma function. Integrating Eq. (B-13) between a specified threshold, T, and infinity provides the probability of false alarm for Λ_{AML} as a function of T. The integration can be performed in general by expressing the Bessel functions in an infinite series expansion. However, for the case of M being an even integer, the modified Bessel function can be written in terms of a finite series expansion as shown in [20; 8.468]. Restricting M to be an even integer and performing the integration provides

---

[22] A. Erdely, *Tables of Integral Transforms, Volume I*, McGraw-Hill, 1954.

$$P_{FA}(T) \approx \frac{(N-1)^M}{(2N-4)^{\frac{M-1}{2}}\,\Gamma\left(\frac{M}{2}\right)} \left[\sum_{k=0}^{\frac{M}{2}-1} \frac{\left(\frac{M}{2}-1+k\right)!}{k!\left(\frac{M}{2}-1-k\right)!} \frac{2^{-k-\frac{1}{2}}}{(N-2)^{\frac{M+1}{2}}} \Gamma\left(\frac{M}{2}-k, NT-2T\right) \right.$$

$$\left. + \frac{1}{2} \sum_{k'=0}^{\frac{M}{2}} \frac{\left(\frac{M}{2}+k'\right)!}{k'!\left(\frac{M}{2}-k'\right)!} \frac{2^{-k-\frac{1}{2}}}{(N-2)^{\frac{M+3}{2}}} \Gamma\left(\frac{M}{2}-k'+1, NT-2T\right) - \ldots \right], \tag{B-14}$$

where $\Gamma(,)$ denotes an incomplete gamma function and where for brevity only the first two terms in the asymptotic series are presented. For T small, the first term is larger than the second term by approximately a factor of N, and higher order terms in the series fall off in significance in terms of increasing powers of N. In general, the first term in Eq. (B-14) will be the dominant term provided N is large and T is not allowed to become too large.

GENERALIZED LIKELIHOOD

The noise only density function for

$$\Lambda_{GLR} = \sum_{k=1}^{M} \hat{\gamma}_k^2 \cos^2 \hat{\theta}_k = \sum_{k=1}^{M} \hat{h}_k \;;\; \hat{h}_k = \hat{\gamma}_k^2 \cos^2 \hat{\theta}_k \tag{B-15}$$

could be obtained by following the same techniques as for Λ_{AML}. Here though, the probability density function of $\hat{h}_k$ will first be evaluated directly. The probability density function for $\cos^2 \hat{\theta}_k$ with $\hat{\theta}_k$ uniformly distributed between $-\pi$ and π can be evaluated through the use of [16; 5-6, 5-7], [23; p. 232], and the twice angle formula as

$$p(y) = \frac{1}{\pi} (y-y^2)^{-\frac{1}{2}} \;;\; y = \cos^2 \hat{\theta}_k, 0 < y < 1. \tag{B-16}$$

The probability density function for $\hat{\gamma}_k^2$ can be obtained from [18; 5-15] as

$$p(x) = (N-1)(1-x)^{N-2} \;;\; x = \hat{\gamma}_k^2, 0 < x < 1. \tag{B-17}$$

The probability density function for $\hat{h}_k$ can be evaluated from Eq. (B-16), Eq. (B-17), [16; 7-46], and [21; 212-7a] as

$$p(h_k) = (1-h_k)^{N-2} \sqrt{\frac{1-h_k}{h_k}}, \left[\frac{2^N}{\pi} \frac{(N-1)!}{(1;2;N-1)}\right], \quad 0 < h_k < 1, \tag{B-18}$$

where (a;b;c) denotes a(a+b) (a+2b) ... (a+cb−b). The characteristic function of h_k is then defined by

---

[23] S. Shelby, "Standard Mathematical Tables," The Chemical Rubber Company, 1964.

$$g(u) = \int_0^1 e^{iuh_k} (1-h_k)^{N-2} \sqrt{\frac{1-h_k}{h_k}} \left[\frac{2^N}{\pi} \frac{(N-1)!}{(1;2;N-1)}\right] d\, h_k . \qquad \text{(B-19)}$$

Making the change of variable $h_k = r^2$ leads to

$$g(u) = \left[\frac{2^N}{\pi} \frac{(N-1)!}{(1;2;N-1)}\right] \int_0^1 2(1-r^2)^{N-\frac{3}{2}} e^{iur^2} dr. \qquad \text{(B-20)}$$

Utilizing the same expansion as listed in Eq. (B-6) leads to

$$g(u) = 2\left[\frac{2^N}{\pi} \frac{(N-1)!}{(1;2;N-1)}\right] \int_0^1 \exp\left[-(N-1.5-iu)r^2 - (N-1.5)\sum_{k=2}^{\infty} \frac{r^{2k}}{k}\right] dr. \qquad \text{(B-21)}$$

Making the change of variable $S = r\sqrt{N - 1.5 - iu}$ in Eq. (B-21) and then expanding the higher order exponent terms in separate Taylor series expansions leads to

$$g(u) = \left[\frac{2^N}{\pi} \frac{(N-1)!}{(1;2;N-1)}\right] \frac{2}{\sqrt{N - 1.5 - iu}} \int_0^{\sqrt{N-1.5-iu}} e^{-S^2} \left[1 - \frac{(N-1.5)S^4}{2(N-1.5-iu)^4} - \right.$$

$$\left. \frac{(N-1.5)S^6}{3(N-1.5-iu)^6} + \ldots\right] dS, \qquad \text{(B-22)}$$

where terms inside the brackets have been ordered according to their significance. The approximation to be employed on the characteristic function is to change the upper limit on the integral to infinity. This is essentially the same approximation as employed for Λ_{AML} and requires N to be large for a high degree of accuracy to occur. Carrying out the integration provides the solution

$$g(u) \approx \left[\frac{2^N}{\pi} \frac{(N-1)!}{(1;2;N-1)}\right] [N - 1.5 - iu]^{-1/2} \left[1 - \frac{3}{8} \frac{N-1.5}{(N-1.5-iu)^2} - \right.$$

$$\left. \frac{5}{8} \frac{N-1.5}{(N-1.5-iu)^3} + \ldots\right]. \qquad \text{(B-23)}$$

The characteristic function can now be raised to the M^{th} power and inverted through the use of [22; 3.2.3] in order to obtain the noise only density function for Λ_{GLR}. To simplify the form of the solution, M will once again be restricted to be an even integer. The resulting solution for the density function is

$$p(\Lambda | M, N, \gamma^2=0) \approx \left[\frac{2^N}{\sqrt{\pi}} \frac{(N-1)!}{(1;2;N-1)}\right]^M \frac{\Lambda^{\frac{M}{2}-1}}{\left(\frac{M}{2}-1\right)!} e^{-(N-1.5)\Lambda}$$

$$\left[1 - \frac{3}{2}\frac{(N-1.5)}{(M+2)} \Lambda^2 - \frac{5(N-1.5)}{(M+2)(M+4)} \Lambda^3 + \ldots\right]. \qquad \text{(B-24)}$$

Integrating the density function provides the probability of false alarm expression

$$P_{FA}(T) \sim \left[\frac{2^N}{\sqrt{\pi}} \frac{(N-1)!}{(1;2;N-1)}\right]^M \left[(N-1.5)^{\frac{M}{2}} (N-1)!\right]^{-1} \left[\Gamma\left(\frac{M}{2}, NT-1.5T\right) - \right.$$

$$\left. \frac{1.5}{(N-1.5)(M+2)} \Gamma\left(\frac{M}{2}+2, NT-1.5T\right) + \ldots\right]. \qquad \text{(B-25)}$$

Equation (B-25) possesses the same properties as Eq. (B-14); the first term in the series is the dominant term, provided N is large and T is not allowed to become too large.

APPENDIX C
DEFLECTION RATIOS

A simple technique for examining the detection capability of an algorithm is to calculate its deflection ratio: the mean output with signal present divided by the output standard deviation with noise only present. This ratio is a measure of the signal-to-noise ratio at the output of the processor. For a Gaussian sample statistic at the output of the processor, the deflection ratio determines the Receiver Operating Characteristics of the processor. For a non-Gaussian sample statistic at the output of the processor, the deflection ratio can only be used as a measure of effectiveness without relating it directly to the probability of detection. Here, the deflection ratio for the low coherence form of Λ_{AML} and a normalized cross-correlation will be examined. The standard deviation of Λ_{AML} with noise only present can be calculated through the use of Eq. (27) as

$$\sigma = \frac{\sqrt{M}}{\sqrt{N(N+1)}} \approx \frac{\sqrt{M}}{N} \tag{C-1}$$

where M and N represent the number of frequency intervals and the number of transforms in each frequency region, respectively. The mean level with signal present can also be determined from Eq. (27) but the resulting series expression prevents simple analysis. The mean level is approximately given by

$$\mu \approx \sum_{k=1}^{M} \gamma_k^2 , \tag{C-2}$$

where the γ_k^2's are the true coherence levels in each frequency region. This expression will slightly underestimate the true mean by ignoring the bias present on the sampled values of $\hat{\gamma}_k^2 \cos \hat{\theta}_k$, but is sufficient for the purpose at hand. The deflection ratio for Λ_{AML} is then given by

$$\text{d.r.}\left(\Lambda_{AML}\right) \approx \frac{N \sum_{k=1}^{M} \gamma_k^2}{\sqrt{M}} . \tag{C-3}$$

The deflection ratio for a normalized cross-correlation processor needs to be calculated with an input of N × M transforms, the same number as input to Λ_{AML}. The deflection ratio for a squared, normalized cross-correlation processor* can be obtained from Ref. 18 as

$$\text{d.r.}\ (\rho^2) \approx NM\, \rho^2 \tag{C-4}$$

where ρ^2 represents the magnitude squared coherence across the entire input bandpass. Once again, the bias on the mean of ρ^2 is being ignored. If both low input signal-to-noise

*Although a squared cross-correlation is being utilized here, the comparison results are essentially independent of whether a cross-correlation or a squared cross-correlation is used. A squared cross-correlation is being used because its deflection ratio has the same dimensionality with respect to the input signal-to-noise ratio as Λ_{AML}.

ratio and equal signal-to-noise ratio at each sensor are assumed, Eqs. (C-3) and (C-4) can be written as

$$\text{d.r.}\,(\Lambda_{AML}) \approx \frac{N}{\sqrt{M}} \sum_{k=1}^{M} \left(\frac{S_k}{\eta_k}\right)^2 \tag{C-5}$$

$$\text{d.r.}\,(\rho^2) \approx NM\left(\frac{S_T}{\eta_T}\right)^2 , \tag{C-6}$$

where S_T/η_T represents the input signal-to-noise ratio across the entire bandpass and S_k/η_k represents the input signal-to-noise ratio in each of the M frequency regions. Two scenarios will be examined with the deflection ratios, flat signal spectral levels across the bandpass and the signal occupying only $1/M^{th}$ of the input bandpass. For the case of flat spectral properties across the input bandpass and of signal-to-noise ratio S/η, the deflection ratios are given by

$$\text{d.r.}\,(\Lambda_{AML}) \approx \sqrt{M}\, N\left(\frac{S}{\eta}\right)^2 \tag{C-7}$$

$$\text{d.r.}\,(\rho^2) \approx MN\left(\frac{S}{\eta}\right)^2 . \tag{C-8}$$

For the case of the signal occupying only $1/M^{th}$ of the input bandpass and with a signal-to-noise ratio within that region of S/η, the deflection ratios are

$$\text{d.r.}\,(\Lambda_{AML}) \approx \frac{N}{\sqrt{M}} \left(\frac{S}{\eta}\right)^2 \tag{C-9}$$

$$\text{d.r.}\,(\rho^2) \approx NM\left(\frac{1}{M}\,\frac{S}{\eta}\right)^2 = \frac{N}{M}\left(\frac{S}{\eta}\right)^2 \tag{C-10}$$

Equations (C-7) through (C-10) show when processing gain can be expected from the likelihood expression. For the case of flat signal spectral properties across the input bandpass, the deflection ratio of the likelihood expression is lower by a factor of $\sqrt{M}$. For the case of the signal occupying only $1/M^{th}$ of the input bandpass, the deflection ratio of the likelihood expression is greater by a factor of $\sqrt{M}$.